Computation and Verification of Spectra for Non-Hermitian Systems

Catherine Drysdale [*]
SMS, Lancaster University, MARS, Lancaster, LA1 4YF, United Kingdom

Matthew Colbrook [†]
DAMTP, University of Cambridge, Cambridge, CB3 0WA, United Kingdom

Michael T. M. Woodley [‡]
Department of Physics, University of Bath, Bath, BA2 7AY, United Kingdom

(Received 21 October 2024; revised 2 July 2025; accepted 29 September 2025; published 22 October 2025)

We establish a connection between quantum mechanics and computation, revealing fundamental limitations for algorithms computing spectra, especially in non-Hermitian settings. Introducing the concept of locally trivial pseudospectra, we show such assumptions are necessary for spectral computation. Locally trivial pseudospectra adapt dynamically to system energies, enabling spectral analysis across a broad class of challenging non-Hermitian problems. Exploiting this framework, we overcome a longstanding obstacle by computing the eigenvalues and eigenfunctions of the imaginary cubic oscillator $H_{\mathrm{B}} = p^2 + ix^3$ with error bounds and no spurious modes—yielding, to our knowledge, the first such error-controlled result. We confirm, for instance, the 100th eigenvalue as 627.694712248436511352673702901153 6…. Here, truncation-induced $\mathcal{PT}$-symmetry breaking causes spurious eigenvalues—a pitfall our method avoids, highlighting the link between truncation and physics. Finally, we illustrate the approach's generality via spectral computations for a range of physically relevant operators. This Letter provides a rigorous framework linking computational theory to quantum mechanics and offers a precise tool for spectral calculations with error bounds.

DOI: 10.1103/hf8s-v93b

Among the axioms of quantum mechanics [1,2], Hermiticity of Hamiltonians stands out as mathematical rather than physical. While this condition ensures that eigenvalues of observables are real, it is sufficient rather than necessary. In [3], Bender and Boettcher analyzed eigenvalues of the imaginary cubic oscillator

$$H_{\mathrm{B}} = p^2 + ix^3. \tag{1}$$

Remarkably, H_{B} is not Hermitian, yet has a real, discrete, and bounded-below spectrum [4,5]. This Hamiltonian is also connected to fascinating physical properties via a more general Lagrangian formulation in scalar quantum field theory, such as $\mathcal{L} = \frac{1}{2}(\partial\phi)^2 + \frac{1}{2}m^2\phi^2 - g(i\phi)^N$ $(N \geq 2)$ [6], that can allow for asymptotic freedom where conventional theories lack it [7,8]. Implications for supersymmetry [9] and the Higgs boson [7] have been investigated. Moreover, $\mathcal{PT}$-symmetric quantum electrodynamics has been introduced as an analog of the imaginary cubic field theory $(N = 3)$ [10], following earlier work on calculating the fine structure constant [6].

Research on non-Hermitian quantum systems has flourished, supported by a robust complex extension of quantum mechanics [11–13]. There have been extensive experimental studies across electromagnetism [14–22], acoustics [23,24], electronics [25–29], mechanical systems [30], metamaterial design [31], bound states in the continuum and quantum scattering [32], solitons in wave optics [33] and transitions in optical structures [34–36]. The intersection of non-Hermiticity with topology is a major source of recent interest, and encompasses phenomena that include edge states [37], defect states [38], exceptional rings [39], superconductivity [40], and novel singularities [41], in addition to providing new system classification schemes [42,43].

Eigenvalues are crucial in physical applications of non-Hermitian systems. Systems associated with gain (due to energy sources) and loss (due to the environment) have coupled eigenvalue pairs [14,44], where a perturbation to one results in a change in the other, allowing robustness. This is particularly useful in laser technology [45,46], where optical loss can lead to poor beam quality, and in wireless power transfer [47], where it is important to maintain transfer efficiency. Additionally, non-Hermitian

[*]Contact author: c.drysdale@lancaster.ac.uk
[†]Contact author: mjc249@cam.ac.uk
[‡]Contact author: mw2970@bath.ac.uk

Published by the American Physical Society under the terms of the Creative Commons Attribution 4.0 International license. Further distribution of this work must maintain attribution to the author(s) and the published article's title, journal citation, and DOI.

systems can exhibit exceptional points, with applications in sensing [48,49].

Eigenvalues also underpin the foundations of $\mathcal{PT}$-symmetric quantum mechanics. A Hamiltonian H is $\mathcal{PT}$-symmetric if it is invariant under the combined parity $(p \mapsto -p, x \mapsto -x)$ and time-reversal $(p \mapsto -p, x \mapsto x, i \mapsto -i)$ operators. If H has unbroken $\mathcal{PT}$ symmetry, it has $\mathcal{CPT}$ symmetry for a hidden symmetry $\mathcal{C}$ [50,51]. The dynamics are unitary with respect to a $\mathcal{CPT}$ inner product $\langle f, g\rangle_{\mathcal{CPT}} = \langle \mathcal{CPT} f, g\rangle$. The development of this theory is analogous to the problem that Dirac encountered in formulating the spinor wave equation in relativistic quantum theory. However, one must first find the eigenstates of H to define $\mathcal{C}$ and the physical Hilbert space [52]. Hence, $\mathcal{PT}$-symmetric quantum mechanics is a bootstrap theory: $\mathcal{C}$ is spectrally determined and accurately calculating eigenvalues is essential.

Computing eigenvalues of non-Hermitian operators is notoriously difficult. Previous approaches for H_{B}, such as direct integration [3], domain truncation [53], variational saddle points [54], perturbation theory [52,55], and coupled moment problems [56], lack explicit error bounds. Truncation to finite-dimensional problems often introduces spurious eigenvalues (see Fig. 2). Addressing this remains a key open problem in non-Hermitian quantum mechanics.

Recent work in computability theory has focused on determining whether algorithms can compute spectra for broad classes of operators. This has culminated in the solvability complexity index hierarchy [57–59], which classifies algorithmic limits for spectral computations. Notably, recent efforts have targeted non-Hermitian spectral problems [60].

This Letter addresses the challenges of computing spectra for a broad class of non-Hermitian operators, focusing on H_{B}, due to its central role in $\mathcal{PT}$ symmetry and its striking physical implications, particularly in quantum field theory. To overcome these challenges, we introduce the concept of "locally trivial pseudospectra" (LTP). For $\mathcal{PT}$-symmetric operators, LTP exploits the local dependence of $\langle\cdot,\cdot\rangle_{\mathcal{CPT}}$ on the spectral data of H, essentially building local approximations of $\mathcal{C}$. This corresponds to Hilbert spaces that adapt dynamically to observed energy. Moreover, LTP extends beyond $\mathcal{PT}$-symmetric operators—see Fig. 6 for further examples.

We first prove that computing spectra of non-Hermitian operators is generally impossible without two key physical assumptions. The first concerns the interactions of an operator representation, ensuring that $H\psi$ can be computed with error bounds for wave functions ψ. For H_{B}, we achieve this via rectangular truncations of a finite-range representation and explain how to extend the approach to long-range interactions. The second assumption, encoded by LTP, provides local control over the operator's non-Hermiticity, physically related to the $\mathcal{C}$ operator in the case of $\mathcal{PT}$-symmetric systems. Precisely, it bounds the growth of the resolvent norm near the spectrum (we define LTP after some background). By combining control over interaction terms with LTP, we bound the action of $\mathcal{C}$ on subspaces. In this way, LTP connects physics with computation: the ability to compute spectra hinges on foundational quantum-mechanical structure. We then perform the first verified (i.e., with error bounds) computations of eigenvalues and eigenfunctions of H_{B}, using a diffusion semigroup $\exp(-tH_{\mathrm{B}})$ and asymptotics to bound spectral projections and demonstrate LTP. This dynamic perspective generalizes to a broad class of non-Hermitian operators.

This Letter lays the foundation for rigorously verified spectra across a broad class of systems by introducing a new technology in non-Hermitian quantum mechanics. It provides a powerful tool for accurately computing and verifying spectral properties, bridging the gap between physical and computational feasibility. Beyond resolving the spectrum of H_{B}, this Letter has broad implications in physics and applications of spectral computations (further illustrated in the End Matter, e.g., for exceptional points), and has foundational implications in unifying quantum mechanics and computation.

Fundamental limitations of computing spectra—Two major, and separate, challenges in computing a Hamiltonian's spectrum are long-range interactions and non-Hermiticity. To illustrate this, we use the solvability complexity index hierarchy and adopt a general framework for defining computational problems—applicable to all such problems found in physics—and a general algorithm for solving them (see Ref. [61]). A computational problem is defined by a function representing a physical quantity (e.g., spectra), with convergence to a solution measured within a metric space. One must also specify the information available to the algorithm, such as interaction data. This setup allows us to determine whether a convergent sequence of algorithms exists to solve the problem.

Consider a Hamiltonian H with matrix elements $\{h_{ij}\}_{i,j\in\mathbb{N}}$. We seek a sequence of algorithms $\{\Gamma_m\}$ that, given $\{h_{ij}\}$ as input, produce outputs $\Gamma_m(H)$ converging to the spectrum $\mathrm{Sp}(H)$ as $m \to \infty$.

First, let H be Hermitian ($h_{ij} = \overline{h_{ji}}$), composed as a direct sum of smaller Hermitian blocks that may include long-range terms [69–71]—see Fig. 1(a). We prove [61] that (A) no algorithmic sequence can converge to $\mathrm{Sp}(H)$ for all such inputs. The core obstacle, labeled "R1," is the inability to control the presence of long-range terms.

Second, let H be a (possibly non-Hermitian) tridiagonal Hamiltonian ($h_{ij} = 0$ if $|i-j| > 1$), formed as a direct sum of Jordan blocks. We prove [61] that (B) no algorithmic sequence can converge to $\mathrm{Sp}(H)$ for all such inputs. The key issue, labeled "R2," is the uncontrolled blowup of $\|(H - zI)^{-1}\|$ as $z \to \mathrm{Sp}(H)$, a phenomenon unique to non-Hermitian operators.

These computational boundaries are fundamental and hold for *any* algorithm, regardless of the operations used. They also extend to the computation of eigenvectors.

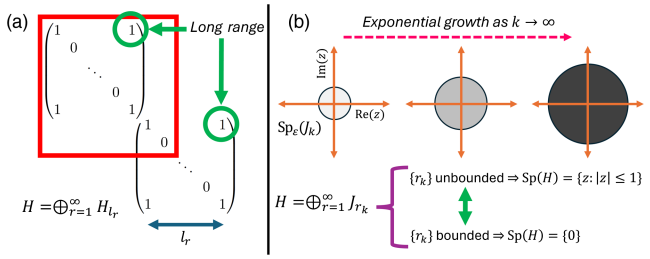

FIG. 1. (a) Illustration of statement (A). We construct direct sums of Hermitian matrices with eigenvalues $\{0, 2\}$ and long-range terms. Block sizes are chosen to "trick" the sequence of algorithms into approximating an eigenvalue 1. The red box shows the information read by the algorithm when making the approximation. (b) Illustration of statement (B). We use direct sums of Jordan matrices whose pseudospectra grow rapidly with size (top panel). By varying block sizes, the algorithm is forced to oscillate (green arrow) between $\{0\}$ (when sizes are bounded) and the unit disk (otherwise).

However, results A and B do not imply that computing $\mathrm{Sp}(H)$ for a specific operator is impossible, only that any method must address R1 and R2.

Introducing LTP to tackle R2—Non-Hermitian properties of a Hamiltonian H can be studied through pseudospectra [72],

$$\mathrm{Sp}_\epsilon(H) \coloneqq \{z \in \mathbb{C} : \|(H - zI)^{-1}\|^{-1} \le \epsilon\}, \quad \epsilon > 0,$$

where $\|(H - zI)^{-1}\|^{-1} = 0$ for $z \in \mathrm{Sp}(H)$. Equivalently, $\mathrm{Sp}_\epsilon(H)$ is the union of $\mathrm{Sp}(H + H')$ for perturbations $\|H'\| \le \epsilon$ [[73], Prop. 4.15]. Hence, $\mathrm{Sp}_\epsilon(H)$ tells us how far an ϵ-sized perturbation can perturb $\mathrm{Sp}(H)$.

To address R2, we use $\|(H - zI)^{-1}\|^{-1}$ to approximate $\mathrm{dist}[z, \mathrm{Sp}(H)]$, the distance from z to the spectrum. For general H, we have $\|(H - zI)^{-1}\|^{-1} \le \mathrm{dist}[z, \mathrm{Sp}(H)]$, with equality when H is Hermitian [74]. For non-Hermitian H, this quantity can significantly underestimate the true distance. If H is quasi-Hermitian, i.e., $H^*\Theta = \Theta H$ for a bounded, positive Hermitian Θ with bounded inverse, then $\mathrm{dist}[z, \mathrm{Sp}(H)] \le \sqrt{\|\Theta\|\|\Theta^{-1}\|}\|(H - zI)^{-1}\|^{-1}$, a condition known as trivial pseudospectrum [75]. In unbroken $\mathcal{PT}$-symmetric cases, this condition corresponds to a bounded transformation between $\langle\cdot,\cdot\rangle$ and $\langle\cdot,\cdot\rangle_{\mathcal{CPT}}$. However, many important non-Hermitian operators, such as H_{B}, do not exhibit trivial pseudospectra [76].

We say an operator H has LTP if, for every compact set $K \subset \mathbb{C}$, there exists $C_K > 0$ such that for all $\epsilon > 0$

$$\mathrm{Sp}_\epsilon(H) \cap K \subset \{z \in \mathbb{C} : \mathrm{dist}[z, \mathrm{Sp}(H)] \le C_K \epsilon\}. \quad (2)$$

This means the pseudospectrum (and thus eigenvalue perturbations) is locally controlled by the distance to the spectrum. For example, if H has a compact resolvent and all eigenvalues are semisimple, then $\|(H - zI)^{-1}\| = \mathcal{O}(1/|z - \lambda|)$ near each eigenvalue λ [[77], Sec. III.6.5]. Since each compact set contains only finitely many such λ,

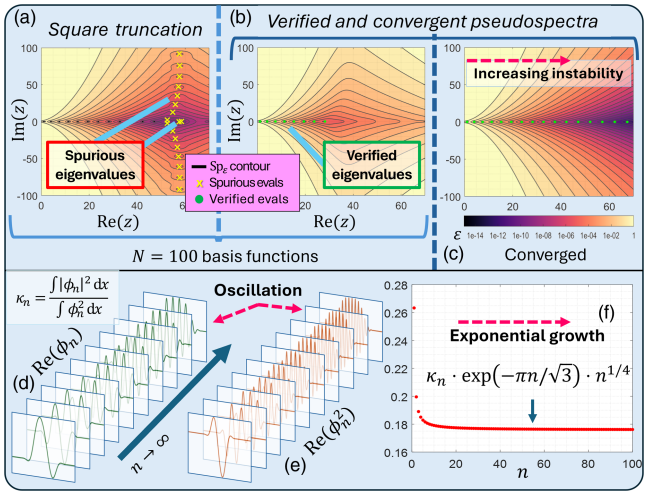

FIG. 2. (a) Pseudospectra approximations via truncated Hermite expansions (square truncations), which break $\mathcal{PT}$ symmetry and produce spurious eigenvalues (yellow crosses). (b),(c) Rectangular truncations preserve $\mathcal{PT}$ symmetry, yield convergent approximations, and remain within the true pseudospectrum. Color indicates $\epsilon = \|(H_{\mathrm{B}} - zI)^{-1}\|^{-1}$. (d),(e) Eigenfunction oscillations. (f) Exponential instability of eigenvalues, with $\lim_{n\to\infty} \kappa_n \exp(-n\pi/\sqrt{3}) n^{1/4} \approx 0.176$.

H satisfies LTP. The concept also extends to operators with continuous spectra, generalizing the stable pseudospectral behavior of Hermitian operators.

For an unbroken $\mathcal{PT}$-symmetric operator H, LTP reflects a locally bounded transformation between $\langle\cdot,\cdot\rangle$ and $\langle\cdot,\cdot\rangle_{\mathcal{CPT}}$. To see this, consider the Riesz projection corresponding to the n th eigenvalue of H, given by

$$\mathcal{Q}_n = \frac{-1}{2\pi i} \int_{S_n} (H - zI)^{-1} dz.$$

Here, the contour S_n wraps once around λ_n and no other eigenvalues [[77], p. 178]. Since each λ_n is simple, the condition number of the eigenvalue λ_n with eigenfunction ϕ_n is (simplifying with $\mathcal{PT}$ symmetry) [78]

$$\kappa_n = \|\mathcal{Q}_n\| = \frac{\langle \phi_n, \phi_n \rangle}{|\langle \mathcal{CPT}\phi_n, \phi_n \rangle|} = \frac{\langle \phi_n, \phi_n \rangle}{\langle \phi_n, \phi_n \rangle_{\mathcal{CPT}}}, \quad \text{and} \quad (3)$$

$$\|(H - zI)^{-1}\| = \kappa_n / \mathrm{dist}(z, \lambda_n) + \mathcal{O}(1), \quad \text{as } z \to \lambda_n, \quad (4)$$

which relates κ_n with the local behavior of $\mathrm{Sp}_\epsilon(H)$.

To compute $\mathrm{Sp}(H_{\mathrm{B}})$, we will determine constants C_K in Eq. (2) for $H = H_{\mathrm{B}}$ and suitable sets K that cover $\mathbb{C}$. Eigenvalues of H_{B} satisfy [3]

$$\lambda_n = \left[\frac{2\Gamma\left(\frac{11}{6}\right)(n - 1/2)\sqrt{\pi}}{\sqrt{3}\Gamma\left(\frac{4}{3}\right)}\right]^{\frac{6}{5}} + \mathcal{O}\left(n^{-4/5}\right), \quad n = 1, 2, \ldots.$$

There exists a constant C_{B} with [79]

$$\lim_{n\to\infty} \kappa_n \exp(-n\pi/\sqrt{3}) n^{1/4} = C_{\mathrm{B}}. \tag{5}$$

Hence, λ_n become exponentially unstable as $n \to \infty$.

Rectangular truncations to tackle R1—We represent H_{B} using Hermite functions $u_m(x) = e^{-x^2/2} H_m(x)$, for $m \in \mathbb{Z}_{\geq 0}$, where $H_m(x)$ is the m th Hermite polynomial. This yields a banded infinite matrix. Panel (a) of Fig. 2 shows pseudospectra of a naive $N \times N$ square truncation, which overestimates pseudospectra and produces spurious eigenvalues, due to neglected interactions with the full system—breaking $\mathcal{PT}$ symmetry.

We instead use *rectangular* truncations [80] (see Fig. 3) to capture the missing interactions, preserve $\mathcal{PT}$ symmetry, overcome R1, and enable verification. Let $\mathcal{P}_N$ be the projection onto $\mathrm{span}\{u_0, \ldots, u_{N-1}\}$. Because of the banded structure of H_{B}, we have $\mathrm{Sp}_\epsilon(H_{\mathrm{B}}\mathcal{P}_N) = \mathrm{Sp}_\epsilon(\mathcal{P}_{N+3} H_{\mathrm{B}} \mathcal{P}_N)$, where the latter is the pseudospectrum of a finite $(N+3) \times N$ matrix that can be computed. This approximation satisfies the bound $\mathrm{Sp}_\epsilon(H_{\mathrm{B}}\mathcal{P}_N) \subset \mathrm{Sp}_\epsilon(H_{\mathrm{B}})$ and converges as $N \to \infty$. Panels (b) and (c) of Fig. 2 illustrate this convergence.

Crucially, rectangular truncations enable approximation of κ_n in Eq. (3). For $z \approx \lambda_n$, the right-singular vector of $\mathcal{P}_{N+3}(H_{\mathrm{B}} - zI)\mathcal{P}_N$ (associated with the smallest singular value) approximates ϕ_n. We compute an initial approximation $\hat{\phi}_n \approx \phi_n$ and verify that $\|\mathcal{P}_{N+3}(H_{\mathrm{B}} - zI)\mathcal{P}_N \hat{\phi}_n\| / \|\hat{\phi}_n\|$ is small using interval arithmetic [61]. Panels (d) and (e) of Fig. 2 show the resulting eigenfunction oscillations; panel (f) confirms Eq. (5), giving $C_{\mathrm{B}} \approx 0.176$.

Calculating the spectrum of H_{B}—To compute the constants C_K in Eq. (2) for $H = H_{\mathrm{B}}$ and address R2 via LTP, we truncate the eigenfunction expansion of $\mathcal{C}$ to $\mathcal{C}_m(x,y) = \sum_{n=1}^{m} \phi_n(x)\phi_n(y)$. From Fig. 2, $\kappa_n \leq \exp(\pi n/\sqrt{3})$, allowing a local bound on the difference between $\langle\cdot,\cdot\rangle$ and $\langle\cdot,\cdot\rangle_{\mathcal{CPT}}$. For $z \in \mathbb{C}\backslash\mathrm{Sp}(H_{\mathrm{B}})$, we bound contributions from eigenvalues $\lambda_n < \mathrm{Re}(z)$ using $\kappa_n/|\lambda_n - z|$, and for $\lambda_n > \mathrm{Re}(z)$, we bound the semigroup generated by $-H_{\mathrm{B}}$ on the corresponding eigenspaces. This requires asymptotic analysis of λ_n to control the tail in $\mathcal{C} \approx \mathcal{C}_m$. The Hille-Yosida theorem [81] then yields a bound on $\|(H_{\mathrm{B}} - zI)^{-1}\|$.

Figure 4 illustrates this argument. The end result (see Ref. [61] for the full proof) is explicit bounds for LTP of H_{B}. Namely, if $\lambda_{m-1} < \mathrm{Re}(z) < \lambda_m$, then

$$\|(H_{\mathrm{B}} - zI)^{-1}\| \leq \frac{\exp\left[(m-1)\frac{\pi}{\sqrt{3}}\right]}{|\lambda_{m-1} - z|} + \frac{\exp\left(m\frac{\pi}{\sqrt{3}}\right)}{|\lambda_m - z|} + c_m, \tag{6}$$

$c_m = \exp\{(m+1)\frac{\pi}{\sqrt{3}} + [2\Gamma(\frac{11}{6})\sqrt{\frac{\pi}{3}}/\Gamma(\frac{4}{3})(m+1)]^{\frac{6}{5}}\}/14$.

Combining this with rectangular truncations (Fig. 3), we can now compute the eigenvalues of H_{B} with explicit error bounds. Figure 5 (top) shows approximations of $\|(H_{\mathrm{B}} - zI)^{-1}\|^{-1}$ using rectangular truncations and $\mathrm{Sp}_\epsilon(\mathcal{P}_{N+3} H_{\mathrm{B}} \mathcal{P}_N)$. As $N \to \infty$, these converge from above and avoid spurious eigenvalues. From Eq. (6),

$$\mathrm{dist}[z, \mathrm{Sp}(H_{\mathrm{B}})] \leq \frac{2\exp\left(m\frac{\pi}{\sqrt{3}}\right)\|(H_{\mathrm{B}} - zI)^{-1}\|^{-1}}{1 - c_m\|(H_{\mathrm{B}} - zI)^{-1}\|^{-1}}. \tag{7}$$

Figure 5 (bottom) shows the effect of this rescaling: the rescaled functions converge to an upper bound on $\mathrm{dist}[z, \mathrm{Sp}(H_{\mathrm{B}})]$, with local minima at the eigenvalues.

We verify eigenvalues in two steps. First, using interval bisection, we locate local minima z_n of the rescaled $\|(H_{\mathrm{B}} - zI)^{-1}\|^{-1}$, obtaining candidate eigenfunctions $\hat{\phi}_n$ from the corresponding right-singular vectors. Equation (6) also predicts the required guard digits. Second, we use

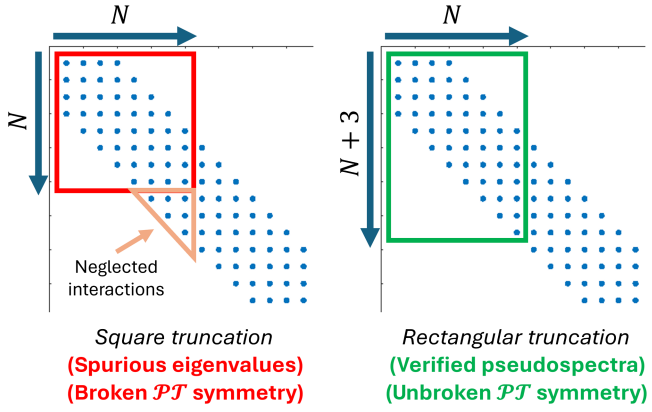

FIG. 3. Left: square truncations of H_{B}'s infinite matrix (blue dots indicate nonzero entries) omit important, physically relevant interactions. A direct check shows that the truncations have broken $\mathcal{PT}$ symmetry. Right: rectangular truncations capture these terms, enabling verified spectra and pseudospectra. Properties of H_{B} (including unbroken $\mathcal{PT}$ symmetry) are preserved under rectangular truncations when we restrict to the subspace (range of $\mathcal{P}_N$).

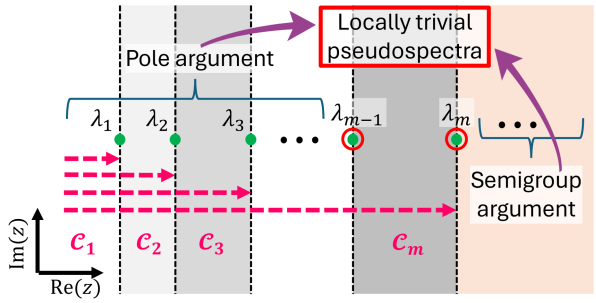

FIG. 4. The proof of Eq. (6) [61] establishes LTP on vertical strips (shaded gray) between eigenvalues. To the left of each strip, we bound eigenvalue contributions using pole bounds $\kappa_m/|\lambda_m - z|$ and truncated operators $\mathcal{C}_m$. To the right, we bound the semigroup generated by $-H_{\mathrm{B}}$. This approach extends to other operators with LTP.

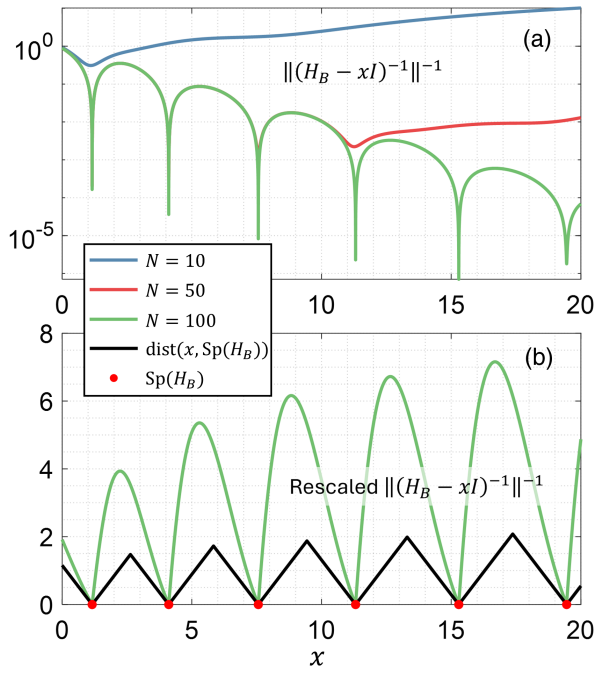

FIG. 5. (a) Approximations of $\|(H_\mathrm{B} - xI)^{-1}\|^{-1}$ using $\mathrm{Sp}_\epsilon(\mathcal{P}_{N+3} H_\mathrm{B} \mathcal{P}_N)$, which converge from above as $N \to \infty$, free of spurious eigenvalues. (b) Rescaled $\|(H_\mathrm{B} - xI)^{-1}\|^{-1}$, which are upper bounds on $\mathrm{dist}[x, \mathrm{Sp}(H_\mathrm{B})]$ used to compute $\mathrm{Sp}(H_\mathrm{B})$ with error bounds.

interval arithmetic to bound $\|(H_\mathrm{B} - z_n I)\hat{\phi}_n\|$, giving a rigorous upper bound on $\|(H_\mathrm{B} - zI)^{-1}\|^{-1}$. Applying Eq. (6) again yields a bound on $|z_n - \lambda_n|$. Verified eigenvalues to 30 digits are shown in Table I. In this manner, we can also compute eigenvectors [61].

Outlook and discussion—We proved that two key physical assumptions are necessary for computing spectra and introduced the concept of LTP. The first assumption, concerning interaction terms, can be enforced via rectangular truncations of Hamiltonians and applies to systems with locally bounded interaction range, yielding sparse matrices. The second addresses non-Hermiticity and is realized through LTP, which is broadly applicable and, in $\mathcal{PT}$-symmetric systems, serves as a local approximation of the hidden symmetry operator $\mathcal{C}$.

As an illustrative example, we computed the first verified eigenvalues of the imaginary cubic oscillator. To address R1, we used rectangular truncations, approximating the spectrum via singular values to avoid spurious modes. To address R2, we demonstrated LTP through asymptotic and semigroup analysis.

The method extends to a wide range of operators, as illustrated by the physically motivated examples in Fig. 6 (End Matter), which exhibit diverse spectral features and highlight the broad applicability of our approach and LTP. For instance, beyond studying H_B on $L^2(\mathbb{R})$, we can consider operators on complex domains, such as those with potentials $x^2(ix)^\nu$ [82], including the upside-down quartic (first row). Additional examples include operators unbounded below (second row), with nonreal spectra (third row), broken $\mathcal{PT}$ symmetry (fourth row), and complex spectra with accumulation points (fifth row). In each case, the Hermite function representation is replaced by another representation to overcome R1.

We can also deal with H that have long-range interactions in two ways. First, by controlling the tail of rectangular truncations, e.g., if hopping terms decay exponentially, one can choose a truncation $\alpha(N)$ such that $\|(I - \mathcal{P}_{\alpha(N)})H\mathcal{P}_N\| \le c_N$ for exponentially decaying c_N, allowing this error to be absorbed into the approximation. An example is given in [61]. Second, we may exploit additional information from the matrix coefficients of H^*H, as in the third row of Fig. 6. We outline the procedure in the End Matter.

We can also generalize Eq. (2) to handle nonsimple eigenvalues by exploiting local algebraic relationships between $\|(H - zI)^{-1}\|^{-1}$ and $\mathrm{dist}[z, \mathrm{Sp}(H)]$, with inversion formulas like Eq. (7). For instance, if an eigenvalue has algebraic multiplicity p, then a higher-order generalization of LTP near that eigenvalue yields

$$\mathrm{Sp}_\epsilon(H) \cap K \subset \{z \in \mathbb{C} : \mathrm{dist}[z, \mathrm{Sp}(H)] \le C_K \epsilon^{1/p}\}. \quad (8)$$

This is particularly useful for analyzing exceptional points, as illustrated in the End Matter.

Additionally, our semigroup approach applies when $\alpha H + \beta I$ generates a strongly continuous semigroup for appropriate scalars α, β. Future work will also explore non-Hermitian operators with continuous spectra [83].

Accurate eigenvalue computations are essential for the stability and efficiency of non-Hermitian systems, as small errors can cause significant deviations in physical behavior and compromise safety. Beyond the applications in the introduction, our method supports optimization in areas such as control for noninvasive imaging and wireless medical devices [84]. Moreover, gain-loss system phenomena extend beyond $\mathcal{PT}$ symmetry. Our approach to accurately compute eigenvalues and eigenvectors enables

TABLE I. Eigenvalues of H_B with absolute error $< 10^{-31}$.

n	Verified eigenvalue λ_n
1	1.156 267 071 988 113 293 799 219 177 999 9
2	4.109 228 752 809 651 535 843 668 478 561 3
3	7.562 273 854 978 828 041 351 809 110 631 4
4	11.314 421 820 195 804 402 233 783 948 426 9
5	15.291 553 750 392 532 388 181 630 791 751 9
6	19.451 529 130 691 728 314 686 111 714 104 4
7	23.766 740 435 485 819 131 558 025 968 789 9
8	28.217 524 972 981 193 297 595 053 878 268 9
9	32.789 082 781 862 957 492 447 371 485 046 3
10	37.469 825 360 516 046 866 428 873 594 530 5
100	627.694 712 248 436 511 352 673 702 901 153 6

analysis of complex systems such as power grids, where balancing supply and demand poses challenges like intermittent generation and the dual roles of energy and information transmission [85,86].

We established a foundational link between quantum mechanics and computation by introducing LTP and proving general limitations on spectral calculations. By understanding these limitations, we overcame them to compute verified eigenvalues of the imaginary cubic oscillator and other non-Hermitian operators. This Letter has both foundational and applied implications for non-Hermitian physics.

Acknowledgments—The authors would like to thank the LMS for the Research in Pairs grant that facilitated the research in this project. M. C. was supported by Isaac Newton Trust Grant No. LEAG/929. We thank the referees for their helpful suggestions and comments.

[1] P. A. M. Dirac, *The Principles of Quantum Mechanics*, 27 (Oxford University Press, New York, 1981).
[2] J. von Neumann, *Mathematical Foundations of Quantum Mechanics* (Princeton University Press, Princeton, NJ, 2018), Vol. 53.
[3] C. M. Bender and S. Boettcher, Phys. Rev. Lett. **80**, 5243 (1998).
[4] P. Dorey, C. Dunning, and R. Tateo, J. Phys. A **34**, 5679 (2001).
[5] E. Caliceti, S. Graffi, and M. Maioli, Commun. Math. Phys. **75**, 51 (1980).
[6] C. M. Bender and K. A. Milton, J. Phys. A **32**, L87 (1999).
[7] C. M. Bender, K. A. Milton, and V. M. Savage, Phys. Rev. D **62**, 085001 (2000).
[8] C. M. Bender, P. N. Meisinger, and H. Yang, Phys. Rev. D **63**, 045001 (2001).
[9] C. M. Bender and K. A. Milton, Phys. Rev. D **57**, 3595 (1998).
[10] C. M. Bender, I. Cavero-Pelaez, K. A. Milton, and K. V. Shajesh, Phys. Lett. B **613**, 97 (2005).
[11] C. M. Bender, D. C. Brody, and H. F. Jones, Phys. Rev. Lett. **89**, 270401 (2002).
[12] C. M. Bender, Rep. Prog. Phys. **70**, 947 (2007).
[13] C. M. Bender, *PT Symmetry: In Quantum and Classical Physics* (World Scientific, Singapore, 2019).
[14] A. Guo, G. J. Salamo, D. Duchesne, R. Morandotti, M. Volatier-Ravat, V. Aimez, G. A. Siviloglou, and D. N. Christodoulides, Phys. Rev. Lett. **103**, 093902 (2009).
[15] C. E. Rüter, K. G. Makris, R. El-Ganainy, D. N. Christodoulides, M. Segev, and D. Kip, Nat. Phys. **6**, 192 (2010).
[16] L. Feng, M. Ayache, J. Huang, Y.-L. Xu, M.-H. Lu, Y.-F. Chen, Y. Fainman, and A. Scherer, Science **333**, 729 (2011).
[17] A. Regensburger, C. Bersch, M.-A. Miri, G. Onishchukov, D. N. Christodoulides, and U. Peschel, Nature (London) **488**, 167 (2012).
[18] L. Xiao, T. Deng, K. Wang, Z. Wang, W. Yi, and P. Xue, Phys. Rev. Lett. **126**, 230402 (2021).
[19] B. Peng, Ş. K. Özdemir, F. Lei, F. Monifi, M. Gianfreda, G. L. Long, S. Fan, F. Nori, C. M. Bender, and L. Yang, Nat. Phys. **10**, 394 (2014).
[20] S. Bittner, B. Dietz, U. Günther, H. L. Harney, M. Miski-Oglu, A. Richter, and F. Schäfer, Phys. Rev. Lett. **108**, 024101 (2012).
[21] F. Zhang, Y. Feng, X. Chen, L. Ge, and W. Wan, Phys. Rev. Lett. **124**, 053901 (2020).
[22] S. Weimann, M. Kremer, Y. Plotnik, Y. Lumer, S. Nolte, K. G. Makris, M. Segev, M. C. Rechtsman, and A. Szameit, Nat. Mater. **16**, 433 (2017).
[23] C. Shi, M. Dubois, Y. Chen, L. Cheng, H. Ramezani, Y. Wang, and X. Zhang, Nat. Commun. **7**, 11110 (2016).
[24] Y. Aurégan and V. Pagneux, Phys. Rev. Lett. **118**, 174301 (2017).
[25] N. Chtchelkatchev, A. A. Golubov, T. I. Baturina, and V. M. Vinokur, Phys. Rev. Lett. **109**, 150405 (2012).
[26] J. Schindler, A. Li, M. C. Zheng, F. M. Ellis, and T. Kottos, Phys. Rev. A **84**, 040101 (2011).
[27] N. Bender, S. Factor, J. D. Bodyfelt, H. Ramezani, D. N. Christodoulides, F. M. Ellis, and T. Kottos, Phys. Rev. Lett. **110**, 234101 (2013).
[28] W. Cao, C. Wang, W. Chen, S. Hu, H. Wang, L. Yang, and X. Zhang, Nat. Nanotechnol. **17**, 262 (2022).
[29] X. Yang, J. Li, Y. Ding, M. Xu, X.-F. Zhu, and J. Zhu, Phys. Rev. Lett. **128**, 065701 (2022).
[30] C. M. Bender, B. K. Berntson, D. Parker, and E. Samuel, Am. J. Phys. **81**, 173 (2013).
[31] C. Li, R. Yang, X. Huang, Q. Fu, Y. Fan, and F. Zhang, Phys. Rev. Lett. **132**, 156601 (2024).
[32] M. B. Soley, C. M. Bender, and A. D. Stone, Phys. Rev. Lett. **130**, 250404 (2023).
[33] Z. H. Musslimani, K. G. Makris, R. El-Ganainy, and D. N. Christodoulides, Phys. Rev. Lett. **100**, 030402 (2008).
[34] Z. Zhang, Y. Zhang, J. Sheng, L. Yang, M.-A. Miri, D. N. Christodoulides, B. He, Y. Zhang, and M. Xiao, Phys. Rev. Lett. **117**, 123601 (2016).
[35] Y. Chong, L. Ge, and A. D. Stone, Phys. Rev. Lett. **106**, 093902 (2011).
[36] L. Xiao *et al.*, Nat. Phys. **13**, 1117 (2017).
[37] A. Banerjee, R. Sarkar, S. Dey, and A. Narayan, J. Phys. Condens. Matter **35**, 333001 (2023).
[38] B. Zeng and T. Yu, Phys. Rev. Res. **5**, 013003 (2023).
[39] E. J. Bergholtz, J. C. Budich, and F. K. Kunst, Rev. Mod. Phys. **93**, 015005 (2021).
[40] D. C. Ohnmacht, V. Wilhelm, H. Weisbrich, and W. Belzig, Phys. Rev. Lett. **134**, 156601 (2025).
[41] Y.-M. Hu, H.-Y. Wang, Z. Wang, and F. Song, Phys. Rev. Lett. **132**, 050402 (2024).
[42] K. Yang, Z. Li, J. L. K. König, L. Rødland, M. Stålhammar, and E. J. Bergholtz, Rep. Prog. Phys. **87**, 078002 (2024).
[43] C.-H. Liu and S. Chen, Phys. Rev. B **100**, 144106 (2019).
[44] R. El-Ganainy, K. G. Makris, M. Khajavikhan, Z. H. Musslimani, S. Rotter, and D. N. Christodoulides, Nat. Phys. **14**, 11 (2018).
[45] L. Feng, Z. J. Wong, R.-M. Ma, Y. Wang, and X. Zhang, Science **346**, 972 (2014).
[46] H. Hodaei, M.-A. Miri, M. Heinrich, D. N. Christodoulides, and M. Khajavikhan, Science **346**, 975 (2014).

[47] S. Assawaworrarit, X. Yu, and S. Fan, Nature (London) **546**, 387 (2017).
[48] P.-Y. Chen and J. Jung, Phys. Rev. Appl. **5**, 064018 (2016).
[49] Z.-P. Liu, J. Zhang, Ş. K. Özdemir, B. Peng, H. Jing, X.-Y. Lü, C.-W. Li, L. Yang, F. Nori, and Y.-x. Liu, Phys. Rev. Lett. **117**, 110802 (2016).
[50] C. M. Bender, P. N. Meisinger, and Q. Wang, J. Phys. A **36**, 1973 (2003).
[51] C. M. Bender, D. C. Brody, and H. F. Jones, Am. J. Phys. **71**, 1095 (2003).
[52] C. M. Bender, D. C. Brody, and H. F. Jones, Phys. Rev. D **70**, 025001 (2004).
[53] S. Bögli, P. Siegl, and C. Tretter, Commun. Part. Differ. Equ. **42**, 1001 (2017).
[54] C. M. Bender, F. Cooper, P. N. Meisinger, and V. M. Savage, Phys. Lett. A **259**, 224 (1999).
[55] A. Mostafazadeh, J. Phys. A **39**, 10171 (2006).
[56] C. Handy, D. Khan, S. Okbagabir, and T. Yarahmad, J. Phys. A **36**, 1623 (2003).
[57] A. C. Hansen, J. Am. Math. Soc. **24**, 81 (2011).
[58] J. Ben-Artzi *et al.*, arXiv:1508.03280.
[59] M. J. Colbrook, The foundations of infinite-dimensional spectral computations, Ph.D. thesis, University of Cambridge, 2020.
[60] S. N. Chandler-Wilde, R. Chonchaiya, and M. Lindner, J. Spectr. Theory **14**, 719 (2024).
[61] See Supplemental Material at http://link.aps.org/supplemental/10.1103/hf8s-v93bfor proofs of the mathematical theorems, further descriptions of the methods, and further computational examples, which includes Refs. [62–68].
[62] T. Kato, J. Phys. Soc. Jpn. **4**, 334 (1949).
[63] S. Zimmermann and U. Mertins, Z. Anal. Anwend. **14**, 327 (1995).
[64] G. R. Barrenechea, L. Boulton, and N. Boussaid, SIAM J. Sci. Comput. **36**, A2887 (2014).
[65] W. H. Press, W. T. Vetterling, S. A. Teukolsky, and B. P. Flannery, *[fifth reference in Supplemental Material not already in paper] Numerical Recipes 3rd Edition: The Art of Scientific Computing* (Cambridge University Press, Cambridge, England, 2007).
[66] P. W. Dondl, P. Dorey, and F. Rösler, Appl. Math. Res. Express **2017**, 271 (2017).
[67] T. D. Tai, J. Differ. Equations **223**, 351 (2006).
[68] E. B. Davies, J. Operator Theory **53**, 225 (2005), https://www.jstor.org/stable/24715654.
[69] L. G. C. Lakkaraju, S. Ghosh, D. Sadhukhan, and A. Sen (De), Phys. Rev. A **106**, 052425 (2022).
[70] Z. Eldredge, Z.-X. Gong, J. T. Young, A. H. Moosavian, M. Foss-Feig, and A. V. Gorshkov, Phys. Rev. Lett. **119**, 170503 (2017).
[71] P. Schauß, M. Cheneau, M. Endres, T. Fukuhara, S. Hild, A. Omran, T. Pohl, C. Gross, S. Kuhr, and I. Bloch, Nature (London) **491**, 87 (2012).
[72] L. N. Trefethen and M. Embree, *Spectra and Pseudospectra* (Princeton University Press, Princeton, NJ, 2005).
[73] S. Roch and B. Silbermann, J. Operator Theory **35**, 241 (1996), https://www.jstor.org/stable/24718872.
[74] E. B. Davies, J. Operator Theory **43**, 243 (2000), https://www.jstor.org/stable/24715241.
[75] D. Krejčiřík, P. Siegl, M. Tater, and J. Viola, J. Math. Phys. (N.Y.) **56**, 103513 (2015).
[76] P. Siegl and D. Krejčiřík, Phys. Rev. D **86**, 121702 (2012).
[77] T. Kato, *Perturbation Theory for Linear Operators* (Springer, Berlin, Heidelberg, 1995), 2nd ed., Vol. 132.
[78] A. Aslanyan and E. B. Davies, Numer. Math. **85**, 525 (2000).
[79] R. Henry, Ann. Henri Poincaré **15**, 2025 (2014).
[80] M. J. Colbrook, B. Roman, and A. C. Hansen, Phys. Rev. Lett. **122**, 250201 (2019).
[81] A. Pazy, *Semigroups of Linear Operators and Applications to Partial Differential Equations* (Springer, New York, 1983), Vol. 44.
[82] C. M. Bender, S. Boettcher, and P. N. Meisinger, J. Math. Phys. (N.Y.) **40**, 2201 (1999).
[83] Z. Wen and C. M. Bender, J. Phys. A **53**, 375302 (2020).
[84] Z. Ye, M. Yang, and P.-Y. Chen, IEEE J. Electromagn. RF Microw. Med. Biol. **6**, 196 (2021).
[85] P. H. Nardelli, N. Rubido, C. Wang, M. S. Baptista, C. Pomalaza-Raez, P. Cardieri, and M. Latva-aho, Eur. Phys. J. Special Topics **223**, 2423 (2014).
[86] S. Galli, A. Scaglione, and Z. Wang, Proc. IEEE **99**, 998 (2011).
[87] E. Benilov, S. O'Brien, and I. Sazonov, J. Fluid Mech. **497**, 201 (2003).
[88] F. Fraternale, L. Domenicale, G. Staffilani, and D. Tordella, Phys. Rev. E **97**, 063102 (2018).
[89] P. Papkovich, Dokl. Acad. Sci. USSR **27**, 334 (1940).
[90] J. Fadle, Ingenieur-Archiv **11**, 125 (1940).
[91] P. Shankar, *Slow Viscous Flows* (World Scientific, Singapore, 2007).
[92] K. G. Makris, R. El-Ganainy, D. N. Christodoulides, and Z. H. Musslimani, Phys. Rev. Lett. **100**, 103904 (2008).
[93] N. Okuma, K. Kawabata, K. Shiozaki, and M. Sato, Phys. Rev. Lett. **124**, 086801 (2020).
[94] A. E. Siegman *et al.*, Mill Valley, CA, vol. 37, p. 169 (1986).
[95] A. Fox and T. Li, Proc. IEEE **51**, 80 (1963).
[96] H. Landau, J. Opt. Soc. Am. **66**, 525 (1976).
[97] L. G. Wright, P. Sidorenko, H. Pourbeyram, Z. M. Ziegler, A. Isichenko, B. A. Malomed, C. R. Menyuk, D. N. Christodoulides, and F. W. Wise, Nat. Phys. **16**, 565 (2020).
[98] M. Nixon, O. Katz, E. Small, Y. Bromberg, A. A. Friesem, Y. Silberberg, and N. Davidson, Nat. Photonics **7**, 919 (2013).
[99] M. J. Colbrook and A. C. Hansen, J. Eur. Math. Soc. **25**, 4639 (2022).

End Matter

We now present additional non-Hermitian examples in Fig. 6, using LTP to compute verified eigenvalues.

The first row of Fig. 6 shows our method applied to an inverted quartic potential. Anharmonic oscillators are widely studied for testing techniques such as perturbation theory, Padé approximations, diagrammatic expansions, and variational or semiclassical methods. The considered model arises in quantum field theory and has been proposed to describe Higgs sector dynamics in the standard model [8]. Here, boundary conditions are imposed not on the real line but on two Stokes sectors of angular width $\pi/3$, adjacent to and below the positive and negative real axes. We set $x = -i\sqrt{1+2is}$ for $s \in \mathbb{R}$ and discretize the transformed problem using Hermite functions and rectangular truncations of the resulting sparse infinite matrix. The eigenvalues are real and positive.

The second row of Fig. 6 presents our method applied to an advection-diffusion operator on the periodic domain $[-\pi, \pi]$. This models the "explosive instability" of a rotating cylinder under gravity, neglecting inertial and capillary effects [87], and belongs to a broader class of non-Hermitian fluid stability problems [88]. We use a

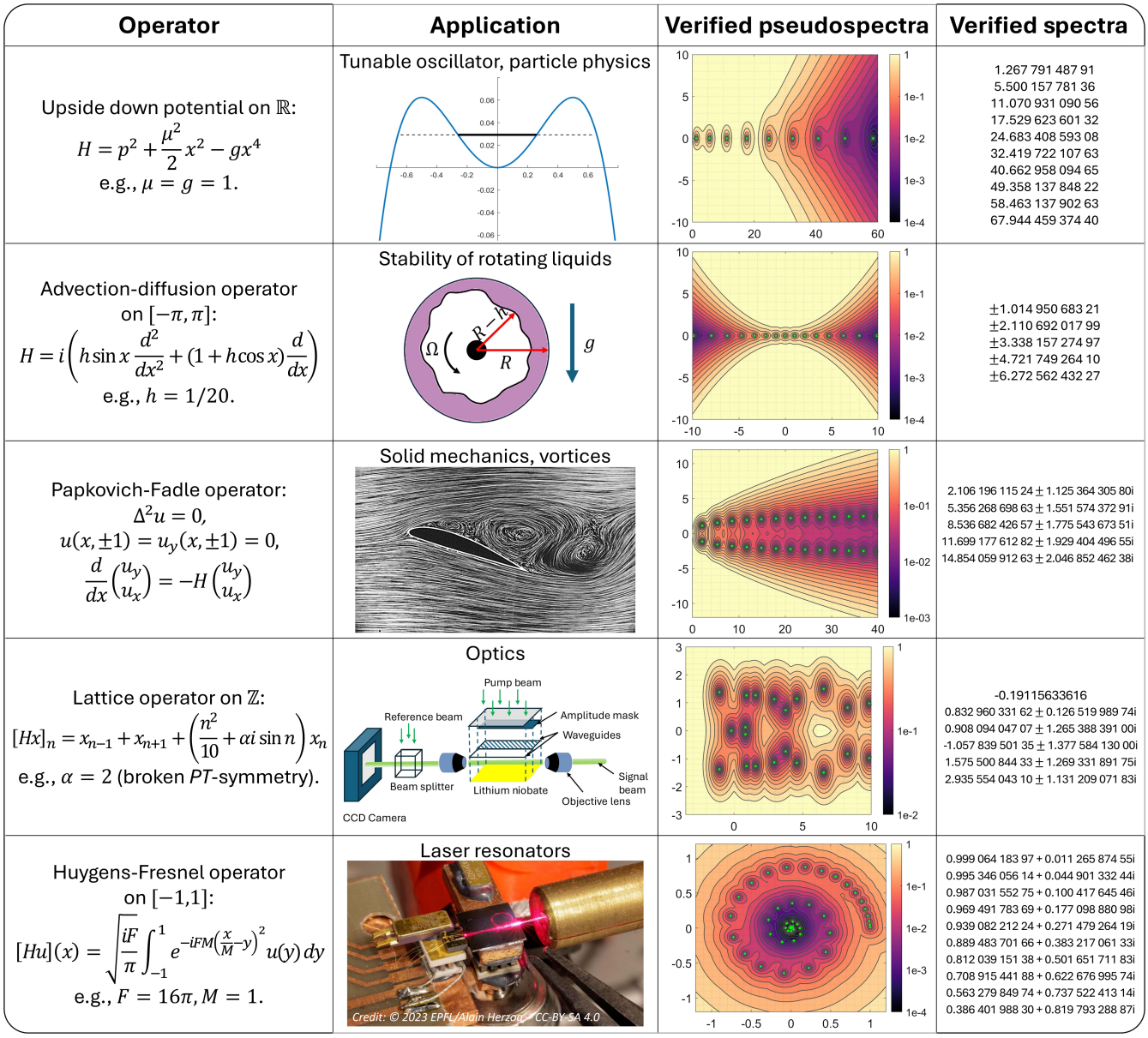

FIG. 6. Examples of other non-Hermitian operators for which we applied our method. In each case, we compute the first 10 nontrivial eigenvalues with verified absolute error $< 10^{-10}$.

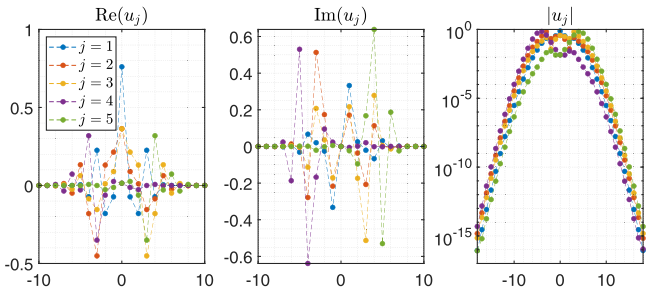

FIG. 7. First five eigenfunctions for the lattice operator (fourth row of Fig. 6) computed with error bounded by 10^{-10}.

Fourier basis and apply rectangular truncations to the resulting sparse infinite matrix. The spectrum consists of real eigenvalues extending to $\pm\infty$.

The Papkovich-Fadle operator, arising in solid and fluid mechanics, concerns solutions u of the biharmonic equation on a semi-infinite strip [89,90]. This operator attracts significant due to the non-normal nature of its eigenfunctions and expansions [91]. We approximate its eigenfunctions using a Chebyshev basis, orthonormalized to form an infinite basis representing the operator. Acting on block-2 functions over $[-1, 1]$, the operator evolves solutions horizontally. Its matrix representation exhibits long-range interactions, so we work with matrices for H and H^*H. Namely, letting σ_{inf} denote the smallest singular value, $\sigma_{\text{inf}}[(H - zI)\mathcal{P}_N] = \sqrt{\sigma_{\text{inf}}[\mathcal{P}_N(H - zI)^*(H - zI)\mathcal{P}_N]}$. The eigenvalues occur in conjugate pairs with increasing imaginary parts.

Open systems often lead to non-Hermitian Hamiltonians due to the lack of energy conservation. Increasing the imaginary part of the potential beyond a critical threshold can trigger a transition from real to complex spectra (symmetry breaking). These phenomena are well studied and experimentally realized in optical systems [14,15,17,45,46,92]. We consider a lattice model on the discrete space $l^2(\mathbb{Z})$, incorporating an aperiodic complex potential superimposed on a harmonic potential. The aperiodicity arises from the incommensurability between the potential and the lattice. Our approach is versatile and capable of handling any type of potential.

In such systems, the spectra of truncated models are often highly sensitive to the imposed boundary conditions, exhibiting phenomena like the non-Hermitian skin effect [93]. The rectangular truncations employed here provide a natural set of boundary conditions that directly approximate the spectra of the infinite lattice model. This approach enables the algorithm to separate bulk states from edge states. In this example, some eigenvalues are real, while others form conjugate pairs. Increasing the value of α increases the imaginary parts of these eigenvalues. The fourth row of Fig. 6 examines the broken $\mathcal{PT}$-symmetric regime.

We can also compute eigenvectors with error bounds (see Ref. [61] for details in the case of the imaginary cubic oscillator). Figure 7 shows the first five eigenvectors computed for $\alpha = 2$. The $\mathcal{PT}$ symmetry enforces specific structures; for instance, the modes with $j = 2$ and $j = 3$ (corresponding to complex-conjugate eigenvalues) have real parts that are reflections of each other and imaginary parts that are negative reflections. As α increases from zero, exceptional points emerge when eigenvalues coalesce and become nonsimple. At these points, the standard LTP no longer holds. However, we can apply the generalized high-order version in Eq. (8) with $p = 2$, corresponding to the algebraic multiplicity. This enables us to compute both eigenvalues and generalized eigenspaces with controlled error, as illustrated in Fig. 8. Notably, we can detect this phenomenon in the bulk, independent of boundary effects.

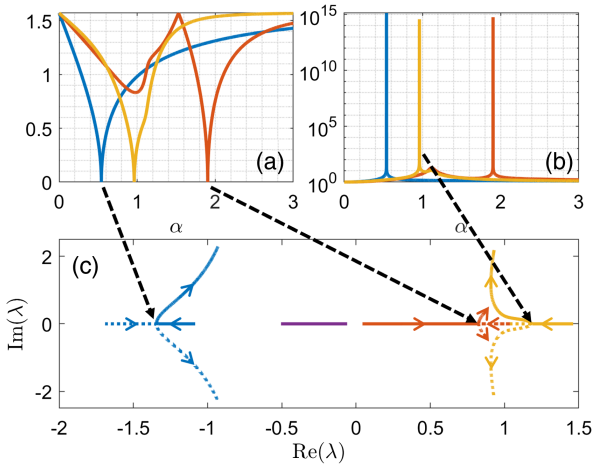

FIG. 8. Exceptional points for lattice operator (Fig. 6, fourth row). (a) Subspace angle between eigenvectors computed with error bounded by 10^{-10}. (b) Enlargement of LTP bound showing the need for higher-order LTP. (c) Trajectory of eigenvalues as α varies, with exceptional points shown by arrows. Dashed and solid lines show eigenvalue pairs that collide.

The final row of Fig. 6 considers an operator modeling a laser resonator with Fresnel number F and magnification

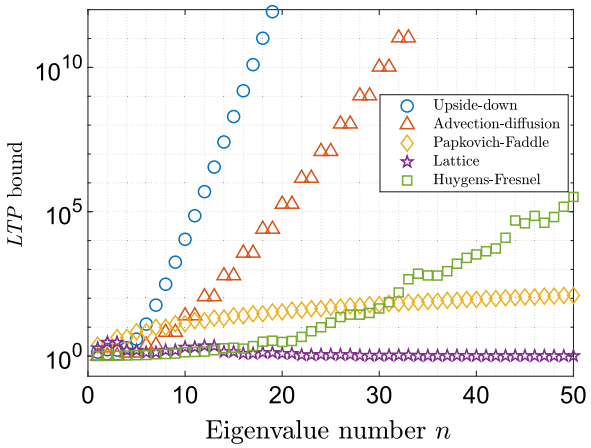

FIG. 9. The constants C_K that locally bound the pseudospectra around each eigenvalue of the operators in Fig. 6.

M, tracing back to work by Siegman *et al.* [94], Fox and Li [95], and Landau [96]. Laser operation involves two key eigenvalue problems: the Hermitian Schrödinger operator governing energy level differences (e.g., the neon frequency gap), and the optical cavity, which resonates at this frequency to produce coherence. The resulting non-Hermitian modes have attracted considerable interest [97,98]. Here, the eigenvalues are complex and spiral inward the accumulation point 0.

To compute verified eigenvalues, Fig. 9 shows the LTP bounds (C_K constants) for the first 50 eigenvalues of each model, ordered by increasing absolute value (decreasing for the Huygens-Fresnel operator). For the upside-down potential, advection-diffusion, and Huygens-Fresnel operators, the bounds grow exponentially with index. For the Papkovich-Fadle operator, growth is algebraic. In the lattice model, the bounds converge to 1, as the unbounded real part of the potential dominates at high energies.